NASA TECHNICAL MEMORANDUM

NASA TM X-73560

NASA TM X-73560

(NASA-TM-X-73560) ACOUSTIC SIGNATURES OF A MODEL FAN IN THE NASA-LEWIS ANECHOIC WIND TUNNEL (NASA) 17 p HC A02/MF A01 CSCL 20A

N77-13792

Unclas
G3/71 58276

ACOUSTIC SIGNATURES OF A MODEL FAN IN THE NASA-LEWIS ANECHOIC WIND TUNNEL

by Donald A. Dietrich, Marcus F. Heidmann,
and John M. Abbott
Lewis Research Center
Cleveland, Ohio 44135

TECHNICAL PAPER to be presented at the
Fifteenth Aerospace Sciences Meeting sponsored by the
American Institute of Aeronautics and Astronautics
Los Angeles, California, January 24-26, 1977

ACOUSTIC SIGNATURES OF A MODEL FAN IN THE NASA-LEWIS ANECHOIC WIND TUNNEL

Donald A. Dietrich,* Marcus F. Heidmann,†
and John M. Abbott††
National Aeronautics and Space Administration
Lewis Research Center
Cleveland, Ohio

Abstract

One-third octave band and narrowband spectra and continuous directivity patterns radiated from an inlet are presented over ranges of fan operating conditions, tunnel velocity, and angle of attack. Tunnel flow markedly reduced the unsteadiness and level of the blade passage tone, revealed the cut-off design feature of the blade passage tone, and exposed a lobular directivity pattern for the second harmonic tone. The full effects of tunnel flow are shown to be complete above a tunnel velocity of 20 meters/second. The acoustic signatures are also shown to be strongly affected by fan rotational speed, fan blade loading, and inlet angle of attack.

E-9002

Introduction

The inability of ground-static acoustic tests to yield turbofan engine fan acoustic characteristics indicative of that which would be measured during flight is well documented. Refs. 1 through 7 all indicate that inflow disturbances present during static tests and absent under flight conditions interact with the rotor to generate tone and broadband noise not present during flight. This noise resulting from the rotor interacting with inflow disturbances tends to mask the benefits attained through design techniques aimed at reducing rotor/stator interaction noise levels. Refs. 8 through 14 attest to the number of investigations that have attempted to eliminate the excess noise in ground based facilities. These attempts have realized varying degrees of success.

An approach to simulating flight conditions is through the use of an anechoic wind tunnel. To this end the NASA-Lewis 9 by 15 low speed wind tunnel has been modified to achieve near anechoic or free-field properties in the test section. The capabilities and limitations of the facility are described in Refs. 1, 15, and 16. Ref. 1, in particular, concludes that the anechoic wind tunnel is a useful facility for applied research on aircraft engine fan noise during flight.

The purpose of this paper is to present representative model fan noise data indicating the type of acoustic information that can be obtained in the NASA-Lewis anechoic wind tunnel. The model fan used for the test is designed to have the blade passage tone cut-off below 107% of the design rotational speed.[1,17,18,19] Where applicable, the results of the test are related to known forward flight effects and to the rotor/stator cut-off theory.[17,18]

One-third octave band and narrowband spectra as well as continuous directivity patterns radiated from an inlet are presented. Data are shown over a range of conditions. The fan operating conditions varied include the rotational speed from 79 to 116% of the design value and the nozzle exit area. The ranges of wind tunnel airflow velocities and inlet angle of attack are zero to 43 m/sec and zero to 30°, respectively.

Apparatus

Anechoic Wind Tunnel

Fig. 1 is a schematic representation of the NASA-Lewis 8- by 6-foot[20] and 9- by 15-foot wind tunnels.[21] The NASA-Lewis anechoic wind tunnel is the terminology used to refer to the combination of the 9- by 15-foot low speed test section, the tunnel drive motors, and enclosed flow path. This facility has been used in the past for reverberant noise measurements as discussed in Refs. 15 and 22 through 30. More recently, however, the wind tunnel has been modified to allow anechoic experimentation in the acoustic direct field within the test section during tunnel operation.

The low speed test section has been used extensively for aerodynamic testing, and its aerodynamic properties are reported in Ref. 21. That report indicates that the test section velocity profile is uniform and the turbulence low. The flow being driven by the compressor circulates in a counter-clockwise direction making two 90° turns prior to reaching the 9- by 15-foot test section. The airflow in the test section is varied by control of both the tunnel drive motor speed and the position of the flow control doors immediately upstream of the test section (Fig. 1). Velocities in the range of 10 to 70 m/sec are established and controlled in this manner. Airflow velocities below 10 m/sec may be induced by the use of auxiliary fans that are normally used for air circulation during air dryer reactivation operations.

Since the original construction, the test section has been modified by the addition of acoustic treatment on the test section walls, floor, and ceiling. The modification of the wind tunnel and the acoustic characteristics of the test section the reported in Refs. 1, 15, and 16. These reports indicate that anechoic or free-field properties exist for frequencies above 1000 hertz. For the purposes of acoustic testing, the entire anechoic wind tunnel has the favorable characteristics of remote drive motors, an acoustical muffler between the compressor and test section, and acoustic treatment on the first turn upstream and downstream of the test section (Fig. 1). With these features the background noise level (one-third octave band) in the test section is 83 dB at 1000 hertz for a 40 m/sec airflow velocity. The background noise level is lower at lower airflow velocities and at higher frequencies.[16] As may be expected, the narrowband (25 Hz bandwidth) background level above

*Aerospace Research Engineer, Wind Tunnel and Flight Division, Member AIAA.

†Aerospace Research Engineer, V/STOL and Noise Division, Member AIAA.

††Aerospace Research Engineer, Wind Tunnel and Flight Division.

STAR Category 71

1000 hertz is at least 10 dB lower than the one-third octave background noise level.

Model Fan and Inlet

The model fan has 15 blades and a diameter of 50.8 cm. The design rotational speed is 8020 rpm which results in a blade passage tone of 2005 hertz. Throughout this paper, the fan rotational speed is expressed in terms of the percentage of the design rotational speed. The aerodynamic performance of the fan (using 11 stator vanes) is reported in Ref. 31. Ref. 32 indicates that the aerodynamic characteristics of the 25-vane configuration used for the present tests are the same as the 11-stator-vane configuration. The rotor-stator spacing is approximately one rotor chord. The fan could be operated to a maximum of 120% of the design rotational speed. At this rotational speed, the fan pressure ratio is approximately 1.25 and the rotor tip speed 256 m/sec. This model is therefore representative of a [illegible] having a low fan pressure ratio and subsonic tip speed.

Some of the acoustic design properties of the fan are discussed in Ref. 1. Of particular importance to this paper are the tone cut-off properties as described in Refs. 17 and 18. For this model fan, which has a stator-vane/rotor-blade ratio of 1.67, the cut-off theory predicts that the fundamental or first harmonic of the blade passage tone will not propagate below 107% of the design speed. This feature of the fan does not consider any effect due to the inlet radius contraction as reported in Ref. 33. According to the cut-off theory the second harmonic tone will propagate at all fan rotational speeds. Propagation of the second harmonic is discussed in Ref. 1 and may be expected to exhibit a distinctively lobed pattern when not masked by extraneous noise sources.

The inlet used during this test is representative of a conventional flight inlet having a low throat Mach number (0.60). The inlet lip geometry is a 2:1 ellipse with an area contraction ratio (highlight-to-throat) of 1.46. The inlet provides very little flow diffusion with a fan-annulus-(diffuser exit) to-throat area ratio of 1.011. Even though the inlet flow diffusion is low, there is an inlet radius contraction at the throat that compensates for the centerbody of the fan. The ratio of inlet-throat-to-fan-tip radii is 0.883. The inlet aerodynamic performance is reported in Ref. 32. At the conditions discussed in this paper paper, the inlet flow is always attached. The inlet total pressure recovery is always above 0.99 and total pressure distortion (maximum minus minimum/average) below 0.02.

The installation of the fan and inlet in the anechoic wind tunnel is shown in Fig. 2. The fan and drive turbine discharge flows are ducted away and turned 90°, pass through an acoustic muffler (Fig. 2(a)), and are exhausted outside the test section.[32] An adjustable plug at the muffler exit allows the remote setting of the nozzle area and thereby the fan operating point. The 90° elbow and vertical duct (Fig. 2(a)) are lined with acoustic treatment to suppress aft fan noise. In addition, the turning vanes in the elbow are acoustically treated to prevent reflection of the aft fan noise upstream. As shown in Fig. 2, inlet angle of attack is varied by rotating the model in the horizontal plane.

Acoustic Instrumentation

The primary piece of acoustic instrumentation is also shown in Fig. 2 and consists of a "sword" microphone and rotating microphone boom. The sword microphone system employs a standard commercially available microphone head (0.635 cm. diam.) with bullet nose. The unique feature of the system is the remote location of the cathode follower which is located in the thickened (vane) portion of the support (Fig. 2(a)). This feature allows a very thin, streamlined microphone system that weathervanes above its support. This is done so that the microphone is always oriented directly into the airflow which is the condition of minimum wind noise on the microphone.

The microphone is located 3.6 fan diameters from the intersection of the fan axis with the inlet highlight plane (Fig. 2(b)). It is mounted on the end of a boom which is capable of being rotated about a vertical axis through the inlet face. By rotating the boom, the microphone can be swept in a circular arc in the horizontal plane at the height of the fan axis.

The electrical signal from the microphone is treated in a conventional manner and recorded on magnetic tape. In addition, the microphone signal is processed through additional amplifiers, filters, and logarithmic converters to yield an on-line (real time) analysis of the acoustic signature. This system provides an on-line plot of the inlet directivity pattern as the microphone boom is remotely rotated.

Test Matrix

Basically the tests were performed over variations in four parameters: the wind tunnel airflow velocity, model fan rotational speed, fan nozzle area, and inlet angle of attack. A fan map which shows the fan operating conditions is presented in Fig. 3. As indicated, the data were obtained along either a fixed operating line (fixed nozzle area for 43 m/sec tunnel velocity) or a fixed rotational speed line.

Along the fixed operating line (circular symbols, Fig. 3), the fan corrected rotational speed was set at 79, 95, 103, 106, 110, and 116% of the design speed. For all of these rotational speeds, data were obtained at wind tunnel airflow velocities of 0, 8, and 43 m/sec and an angle of attack of 0°. For the two rotational speeds of 95 and 116% of design, additional zero angle of attack data were obtained at wind tunnel airflow velocities of 14, 22, and 32 m/sec. For a selected airflow velocity of 43 m/sec, data were obtained at angles of attack of 15° and 30° for the 95 and 116% design speed conditions.

An alternate method of setting the fan operating condition was along a fixed rotational speed line (square symbols, Fig. 3). For a fixed rotational speed of 106% of design, the fan nozzle area was varied to set the operating condition. This was done at a tunnel velocity of 43 m/sec and 0° angle of attack only.

Test Procedure

For each model fan operating condition in the test matrix, the individual conditions were estab-

lished sequantially in the following order: wind tunnel airflow velocity, fan rotational speed, fan mass flow (by adjusting the nozzle area), and finally the inlet angle of attack. Once the desired model operating condition was established, data were obtained with the microphone sweeping a circular arc, the microphone fixed at specified locations, and finally again with the microphone sweeping.

Initially, the microphone was set at a shallow microphone angle as shown in Fig. 2(b) (20° for 0° angle of attack, and 35° for nonzero angles of attack). The microphone angle* was measured with respect to the fan axis in all cases. The microphone angle was then varied at 2.5°/sec to 120° and returned to the initial angle. During the first sweep and return, the one-third octave band sound pressure level was recorded on-line at the frequencies containing the first and second harmonics of the blade passage tone. Data were obtained during both the initial and return sweeps to assure repeatability. After completing the microphone sweep, the microphone was rotated to fixed positions of 30°, 60°, and finally 90° (60° and 90° only for nonzero angles of attack). The unfiltered microphone signal was then recorded on magnetic tape for one minute at each fixed position. These data were used later for one-third octave band and narrowband spectral analysis. Finally, the microphone was again swept a second time in the same manner as described above. In this case, the one-third octave band sound pressure level was recorded on-line at two frequencies which were nonintegral multiples (either 0.7 and 1.4 or 1.5 and 2.5) of the blade passage tone.

Results

This section presents representative examples of the data obtained. Figs. 4 to 6 show typical data for the on-line directivity traces, one-third octave band spectra, and narrowband spectra, respectively. These figures are described briefly here and in more detail in the Discussion of the Results.

On-Line Data

Fig. 4 contains examples of the directivity patterns obtained from the on-line acoustic measurements for a rotational speed of 95% of design and 0° angle of attack. Fig. 4(a) contains data obtained under static (no wind tunnel airflow) conditions while Fig. 4(b) illustrates the results at an airflow velocity of 43 m/sec. The ordinate in each case is the one-third octave band sound pressure level while the abscissa is the microphone angle measured with respect to the fan axis. Data are shown for one-third octave band center frequencies of 1, 2, 0.7, and 1.4 multiples of the blade passage tone, and the range of microphone angles is from 20° to 120°.

One-Third Octave Band Spectra

The data recorded with the microphone in a fixed location were processed on a one-third octave band analyzer using a 4 second integration time. Fig. 5 shows one-third octave band sound pressure level spectra from 1000 to 20 000 Hz for rotational speeds of 79, 95, 106, and 116% of the design speed. The data are shown for 0° angle of attack, for static and 43 m/sec airflow velocity, and for microphone angles of 30°, 60°, and 90°.

Narrowband Spectra

In the same manner as the one-third octave band analysis, the fixed microphone data were processed by the use of a narrow-band (25 Hz bandwidth) analyzer with an approximate integration time of 11 seconds. Fig. 6 shows the narrowband sound pressure level spectra, up to 10 000 hertz, for rotational speed of 79, 95, 106, and 116% of the design speed. The data are shown for 0° angle of attack, for static and 43 m/sec airflow velocity, and for a microphone angle of 60° to the fan axis.

Discussion of the Results

The discussion of the results of this test program are divided into four categories: (1) the effect due to forward velocity, (2) the effect due to fan rotational speed, (3) the effect of fan blade loading, and (4) the effect of inlet angle of attack. It should be kept in mind that the effects enumerated above are in many instances interrelated.

Forward Velocity

One of the effects of airplane forward flight on the engine acoustic signature is the large reduction in tone unsteadiness, as discussed in Ref. 1. The examples of the on-line traces (Fig. 4) indicate this same effect when the data at the static and 43 m/sec airflow conditions are compared. The traces of the first and second harmonics of the blade passage tone show significant reductions in tone unsteadiness (peak-to-valley variation of the trace at any given microphone angle) under wind tunnel flow conditions and become similar in unsteadiness to the broadband noise.

The variation of tone unsteadiness with wind tunnel airflow is shown quantitatively in Fig. 7 for 0° angle of attack, 95% fan rotational speed, and a 60° microphone angle. A measure of the tone unsteadiness is taken to be the maximum peak-to-valley variation in the one-third octave band sound pressure level over a time period of approximately 10 seconds. The unsteadiness of the first and second harmonics of the blade passage tone in decibels is plotted as a function of wind tunnel airflow velocity in m/sec. The inset traces on the figure are representative of the acoustic signatures over a 4 second time interval for wind tunnel airflow velocities of zero and 43 m/sec.

Under static wind tunnel conditions, the sound pressure level unsteadiness of each of the tones is more than 10 dB. At 43 m/sec airflow velocity, the unsteadiness is approximately 3 dB. The decrease in unsteadiness with increasing airflow velocity is monotonic and abrupt with the reduction in unsteadiness being essentially complete by 15 m/sec. It will be shown in the next section that the airflow velocity at which this transition is complete is not always 15 m/sec but is dependent on the model operating conditions.

*For nonzero angles of attack, the microphone angles over which the data are obtained are representative of the forward quadrant below the inlet which, in the case of an aircraft, is the region of interest to a ground observer.

In addition to the reduction in unsteadiness discussed above, comparison of Figs. 4(a) and (b) also shows a large reduction in the sound pressure level of the blade passage tone between the static and wind tunnel flow cases. This effect is expected since the fan is designed to have the blade passage tone cut-off at rotational speeds below the design speed. When the cut-off condition is realized, a blade passage tone is not generated. This design feature in a subsonic tip speed fan has not been directly demonstrated in static test facilities due to a rotor-alone blade passage tone which is generated by the interaction of the fan with the inflow turbulence.[5]

All the parts of Figs. 5 and 6 also indicate a large reduction in the sound pressure level of the blade passage tone once the tunnel flow is established. These figures also indicate the presence of a strong second harmonic of the blade passage tone which at low fan rotational speeds is relatively unaffected by forward velocity.

Figs. 8 and 9 show the effect of forward velocity at 0° angle of attack much more directly. On both figures, the sound pressure levels of the first and second harmonics of the blade passage tone are shown as a function of airflow velocity. The tone levels are determined from the narrowband spectra at the fixed microphone angles of 30°, 60°, and 90° as indicated. Fig. 8 represents the data obtained at a rotational speed of 95% of design while Fig. 9 is done for a speed of 116% of design.

Fig. 8 indicates a monotonic decrease of as much as 20 dB in the sound pressure level of the blade passage tone between zero and 15 m/sec. The level is unchanged above 15 m/sec. This result suggests that the inflow turbulence present at the static condition which causes rotor-alone noise is absent above an airflow of 15 m/sec. The sound pressure level of the second harmonic tone is not cut-off and therefore is comparatively unchanged in level due to forward velocity.

Fig. 9 indicates much the same situation for the higher rotational speed as that of the low rotational speed (Fig. 8). However, the full effect of forward velocity in this case may not be realized until the airflow velocity is 20 m/sec. This result may well be due to the detailed nature of the turbulence present in the test section at static and near-static conditions. However, an alternate possibility exists for the present wind tunnel model installation, Fig. 2(a). The closest obstacle external to the fan which may be the cause of an inflow turbulence is the microphone boom. Such inflow turbulence would cause an increase in the sound pressure level of the blade passage tone. To avoid ingestion of the turbulence caused by the microphone boom the capture streamtube of the inlet flow must be small enough to exclude the boom. For a given fan mass flow (rotational speed), the size of the capture streamtube decreases with increasing tunnel velocity. Thus, below some tunnel velocity the boom turbulence could enter the inlet and cause a blade passage tone; while above that tunnel velocity the boom turbulence would not enter the inlet and the blade passage tone may be absent. This is consistent with data shown in Figs. 8 and 9. Further, the size of the capture streamtube increases with increasing fan mass flow so at higher fan mass flows the tunnel velocity must be greater to keep the capture streamtube small enough to exclude the boom. This is consistent with the higher tunnel velocity at which full blade passage tone reduction is realized at the higher fan speed (Fig. 9, compared with Fig. 8). Finally, if the boom had not been used during the test, the complete effect of forward velocity might have been realized at a tunnel airflow velocity less than 15 m/sec.

Rotational Speed

The most significant effect to be expected due to a change in rotational speed is the change in the acoustic signatures as predicted by the cut-off theory. In particular, at low rotational speeds, the blade passage tone is cut-off, and the second harmonic tone is cut-on. At high rotational speeds both the first and second harmonics should be cut-on. According to the previous discussion, the effect can be observed only with tunnel velocity.

The absence of a blade passage tone at low rotational speeds is shown in Figs. 4, 5(a) and (b), and 6(a) and (b). In particular, the narrowband spectrum of Fig. 6(b) indicates a nearly complete absence of a blade passage tone. These observations verify the predictions of the cut-off theory.

Another feature of the data of Fig. 4(b) is the distinctive lobular directivity pattern of the second harmonic of the blade passage tone. It is notable that this lobular directivity pattern is not exposed until the forward velocity effect is realized as can be seen by comparing the data of Figs. 4(a) and (b). The pattern of Fig. 4(b) is characteristic of the spatial pattern that can be generated by a cut-on rotor/stator interaction. Evidence of these patterns is also shown in Ref. 19. This result coupled with the fact that the directionality of the noise at the blade passage frequency (Fig. 4(b)) has the same basic pattern as that of broadband noise implies that the blade passage tone is cut-off and the second harmonic cut-on at rotational speeds below the design rotational speed.

The data obtained during this test can also be used to determine if the blade passage tone is cut-on at rotational speeds above design. Using Refs. 17 and 18, the blade passage tone should be cut-on at and above rotational speeds of 107% of the design value. However, Ref. 33 states that due to the effect of the inlet radius contraction the cut-on condition forward of the inlet is not realized until a higher rotational speed. Once the blade passage tone is cut-on, the sound pressure level of the tone should increase with respect to both the broadband level and the level of the second harmonic. This effect should first become evident at the microphone position of 90° to the fan axis.

Some indication of a blade passage tone at 116% fan speed is shown in Fig. 5(d) at the 60° and 90° microphone angles and in Fig. 6(d) at the 60° microphone angle. Fig. 10 presents some further information about the nature of the acoustic signatures at a wind tunnel airflow velocity of 43 m/sec and 0° inlet angle of attack. In this figure, the sound pressure levels of the first and second harmonics of the blade passage tone are shown as a function of rotational speed. The sound pressure levels are determined from the narrowband spectra for the fixed microphone positions of 30°,

60°, and 90°.

The data of Fig. 10 show several remarkable features. First, the blade passage tone does not increase dramatically with increasing fan rotational speed as one might expect. Some increase in the blade passage tone level (with respect to the second harmonic tone and broadband levels) is observed at the 60° and 90° microphone angles where the increase would first be expected to be observed. This lack of a dramatic increase in the blade passage tone may be due in part to the inlet radius contraction,[33] and a more detailed study of the inlet-fan combination is required. Second, at particular microphone angles and fan speeds, the second harmonic tone level decreases to the value of the blade passage tone level and close to that of the broadband level. These low values of the second harmonic tone level may be associated with a minimum in the lobular directivity patterns such as those evident in Fig. 4(b).

Blade Loading

The fan map (Fig. 3) shows the various fan operating points for which data were obtained at a constant rotational speed. By varying the nozzle area while maintaining a rotational speed of 106% of the design value, various conditions of fan mass flow and fan pressure ratio are established. These changes result in significant differences in the fan blade loading and the duct Mach number. The fan blade loading parameter used in this paper is the ratio of the total pressure rise across the fan and the flow dynamic pressure relative to the blade at the tip of the fan. The values of the above parameters are presented in the table in Fig. 11.

The curves of Fig. 11 show the resulting acoustic directionality patterns of the tones and broadband noise for the two extreme conditions on the speed line and one intermediate case (points a, b, and c on Fig. 3) for a wind tunnel airflow velocity of 43 m/sec and 0° angle of attack. The curves shown on Fig. 11 are obtained from the on-line directionality traces of the one-third octave band sound pressure level as illustrated in Fig. 4. In general, there is an increase in both the tone and broadband sound pressure levels with increased blade loading; that is, as the fan weight flow is reduced and the fan pressure ratio is increased. This effect agrees with other results that have shown an increase in noise level with increased blade loading.[34,35] In addition, there is a large effect on the directivity pattern of the second harmonic of the blade passage tone as the blade loading is increased. Between microphone angles of 20° and 70°, there is a lobular directionality pattern that becomes increasingly distinct.

Angle of Attack

The effect that inlet angle of attack can have on inlet acoustic directivity is shown in Fig. 12 for an airflow velocity of 43 m/sec, and a fan rotational speed of 95%. The figure is constructed in the same manner as Figs. 4 and 11 with directivity patterns shown for angles of attack of 0°, 15°, and 30°. Clearly in this particular example there is an increase in the sound pressure level of the blade passage tone and broadband noise as the angle of attack is increased. The inlet angle of attack also has a very large effect on the second harmonic tone. Any increase in sound power level is difficult to identify, but there is a significant shift in the directionality pattern of the sound pressure level. The change in the angle of maximum sound pressure level of the directivity pattern is particularly important to the case of an aircraft because both the level and angular direction (with respect to the aircraft) of the maximum perceived noise on the ground can be affected.

Angle of attack can affect the noise in several ways. First, the nonuniform velocity profile at the inlet face when the inlet is at a nonzero or upward angle of attack can cause the noise to be refracted downward. Second, any modification or nonuniformity of the flow at the fan face including the boundary layer can change the character and increase the level of the generated noise. Either or both of these angle of attack effects could cause the observed changes in level and directionality. The changes in the sound pressure level or acoustic patterns cannot be attributed to an inlet flow separation since Ref. 32 has shown that the flow remains attached over these ranges of angle of attack and fan mass flow.

Summary of Results

The acoustic signatures of a model fan in the NASA-Lewis anechoic wind tunnel are discussed. The model fan is designed to have the blade passage tone cut-off for rotational speeds below 107% of the design speed. The data presented are one-third octave band and narrowband spectra and continuous on-line traces of the directivity patterns radiated from an inlet over ranges of fan operating conditions, wind tunnel airflow velocity, and inlet angle of attack. The major results of this paper may be summarized as follows:

1. Presence of a wind tunnel flow velocity greater than approximately 20 m/sec results in a large reduction in both the unsteadiness and level of the sound pressure level of the blade passage tone compared to the static (no wind tunnel airflow) condition.

2. The airflow velocity at which the full forward velocity effect is achieved is related to the amount of flow through the inlet and the location of any flow disturbing device external to the inlet.

3. The cut-off design feature of the model fan is revealed by the absence of a blade passage tone and the distinctive lobular acoustic directivity pattern of the second harmonic of the blade passage tone at forward velocity conditions.

4. Changes in the fan weight flow, fan pressure ratio, fan blade loading, or inlet angle of attack strongly affect the acoustic signatures.

5. It is difficult to isolate the effects of the various fan and wind tunnel operating conditions tested. As of this time, all aspects of the acoustic signatures have not been explained entirely by the effects of inflow turbulence (rotor-alone noise) and rotor/stator interaction noise. A more detailed study of the acoustic characteristics of this fan/inlet combination is required.

References

1. Heidmann, M. F.; and Dietrich, D. A." Simulation of Flight-Type Engine Fan Noise in the NASA-Lewis 9x15 Anechoic Wind Tunnel," NASA TM X-73540, 1976, NASA.

2. Povinelli, F. P., Dittmar, J. H., and Woodward, R. P., "Effects of Installation Caused Flow Distortion on Noise from a Fan Designed for Turbofan Engines," TN D-7076, 1972, NASA.

3. Hanson, D. B., "A Study of Subsonic Fan Noise Sources," AIAA Paper 75-469, Hampton, Va., 1975.

4. Hansen, D. G., "Spectrum of Rotor Noise Caused by Atmospheric Turbulence," Journal of the Acoustical Society of America, Vol. 55, 1974, pp. S3-S4.

5. Heidmann, M. F., "An Observation on Tone Cut-Off in Static Test Data From Jet Engine Fans," TM X-3296, 1975, NASA.

6. Merriman, J. E. and Good, R. C., "Effect of Forward Motion on Fan Noise," AIAA Paper 75-464, Hampton, Va., 1975.

7. Pickett, G. F., "Effects of Non-Uniform Inflow on Fan Noise," presented at the 87th Acoustical Society of America Meeting, New York City, N.Y., Apr. 1974.

8. Cumpsty, M. A. and Lowrie, B. W., "The Cause of Tone Generation by Aero-Engine Fans at High Subsonic Tip Speeds and the Effect of Forward Speed," ASME Paper 73-WA/GT-4, Detroit, Mich., 1973.

9. Roundhill, J. P. and Schaut, L. A., "Model and Full-Scale Test Results Relating to Fan-Noise In-Flight Effects," AIAA Paper 75-465, Hampton, Va., 1975.

10. Lowrie, B. W., "Simulation of Flight Effects on Aero Engine Fan Noise," AIAA Paper 75-463, Hampton, Va., 1975.

11. Hodder, B. K., "The Effects of Forward Speed on Fan Inlet Turbulence and Its Relation to Tone Noise Generation," TM X-62381, 1974, NASA.

12. Hodder, B. K., "An Investigation of Possible Causes for the Reduction of Fan Noise in Flight," AIAA Paper 76-585, Palo Alto, Calif., 1976.

13. Hodder, B. K., "Investigation of the Effect of Inlet Turbulence Length Scale on Fan Discrete Tone Noise," TM X-62300, 1973, NASA.

14. Feiler, C. E. and Merriman, J. E., "Effects of Forward Velocity and Acoustic Treatment on Inlet Fan Noise," AIAA Paper 74-946, Los Angeles, Calif., 1974.

15. Diedrich, James H. and Luidens, Roger W., "Measurement of Model Propulsion System Noise in a Low-Speed Wind Tunnel," AIAA Paper 76-91, Washington, D.C., 1976.

16. Rentz, P. E., "Softwall Acoustical Characteristics and Measurement Capabilities of the NASA Lewis 9x15 Foot Low Speed Wind Tunnel," BBN-3176, June 1976, Bolt, Beranek and Newman, Inc.; also NASA CR-135026.

17. Tyler, J. M. and Sofrin, T. G., "Axial Flow Compressor Noise Studies," SAE Transactions, Vol. 70, 1962, pp. 309-332.

18. Sofrin, Thomas G. and McCann, John C., "Pratt and Whitney Aircraft Experience in Compressor-Noise Reduction," Journal of the Acoustical Society of America, Vol. 40, 1966, pp. 1248-1249.

19. Cumpsty, N. A., "Tone Noise from Rotor/Stator Interactions in High Speed Fans," Journal of Sound and Vibration, Vol. 24, 1972, pp. 393-409.

20. Swallow, R. J. and Aiello, R. A., "NASA-Lewis 8- by 6-Foot Supersonic Wind Tunnel Facility Description with Performance Data," TM X-71542, 1974, NASA.

21. Yuska, J. A., Diedrich, J. H., and Clough, N., "Lewis 9- by 15-Foot V/STOL Wind Tunnel," TM X-2305, 1971, NASA.

22. Loeffler, I. J., Lieblein, S., and Stockman, N. O., "Effect of Rotor Design Tip Speed on Noise of a 1.21 Pressure Ratio Model Fan Under Static Conditions," ASME Paper 73-WA/GT-11, Detroit, Mich., 1973.

23. Piersol, A. G. and Rentz, P. E., "Utilization and Enhancement of the NASA-Lewis 9x15 Foot V/STOL Wind Tunnel for Inlet Noise Research," BBN-2743, May 1974, Bolt, Beranek, and Newman, Inc.

24. Wesoky, H. L.; et al., "Low-Speed Wind Tunnel Tests of a 50.8 cm. (20-in.) 1.15-Pressure-Ratio Fan Engine Model," TM X-3062, 1974, NASA.

25. Miller, B. A. and Abbott, J. M., "Aerodynamic and Acoustic Performance of Two Choked-Flow Inlets Under Static Conditions," TM X-2629, 1972, NASA.

26. Miller, B. A. and Abbott, J. M., "Low-Speed Wind-Tunnel Investigation of the Aerodynamic and Acoustic Performance of a Translating-Centerbody Choked Flow Inlet," TM X-2773, 1973, NASA.

27. Abbott, J. M., Miller, B. A., and Golladay, R. L., "Low-Speed Wind-Tunnel Investigation of the Aerodynamic and Acoustic Performance of a Translating-Grid Choked-Flow Inlet," TM X-2966, 1974, NASA.

28. Miller, B. A., Dastoli, B. J., and Wesoky, H. L., "Effect of Entry-Lip Design on Aerodynamics and Acoustics of High-Throat-Mach-Number Inlets for the Quiet, Clean, Short-Haul Experimental Engine," TM X-3222, 1975, NASA.

29. Abbott, J. M., "Aeroacoustic Performance of Scale Model Sonic Inlets," AIAA Paper 75-202, Pasadena, Calif., 1975.

30. Rentz, E., "Hardwall Acoustical Characteristics and Measurement Capabilities of the NASA-Lewis 9x15 Low Speed Wind Tunnel," BBN-3174, June 1976. Bolt, Beranek, and Newman, Inc.; also NASA CR-135025.

31. Lewis, G. W., Jr. and Tysl, E. R., "Overall and Blade-Element Performance of a 1.20-Pressure-Ratio Fan Stage at Design Blade Setting Angle," NASA TM X-3101, 1974.

32. Abbott, John M.; Diedrich, James H.; and Williams, Robert C.: Low Speed Aerodynamic Performance of 50.8-Centimeter-Diameter Noise Suppressing Inlets for the Quiet, Clean, Short-Haul Experimental Engine (QCSEE). NASA TM X to be published.

33. Mathews, D. C. and Nagel, R. T., "Inlet Geometry and Axial Mach Number Effects on Fan Noise Propagation," AIAA Paper 73-1022, Seattle, Wash., 1973.

34. Feiler, C. E. and Conrad, William, "Noise from Turbomachinery," AIAA Paper 73-815, St. Louis, Mo., 1973.

35. Heidmann, M. F. and Feiler, C. E., "Noise Comparisons From Full-Scale Fan Tests at NASA-Lewis Research Center," AIAA Paper 73-1017, Seattle, Wash., 1973.

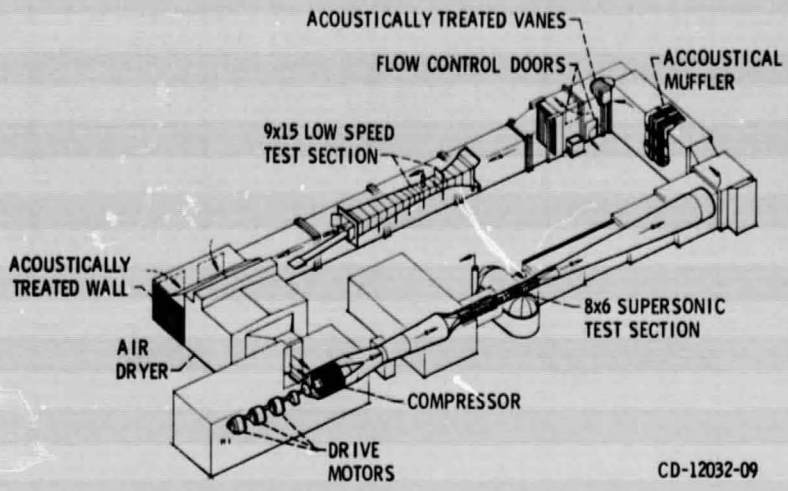

Figure 1. - The NASA-Lewis 8- by 6-foot and 9- by 15-foot wind tunnels.

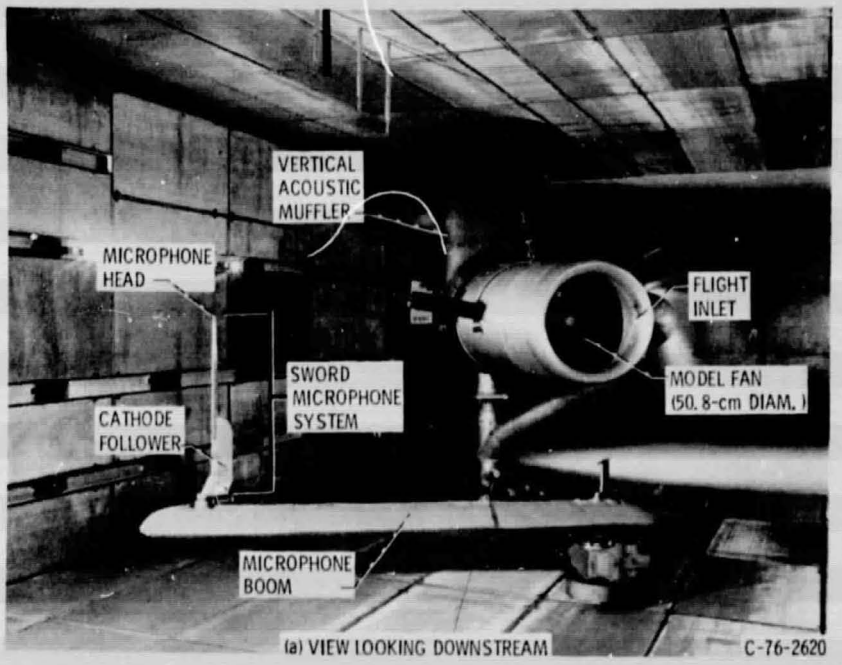

Figure 2. - Model fan installed in the anechoic wind tunnel.

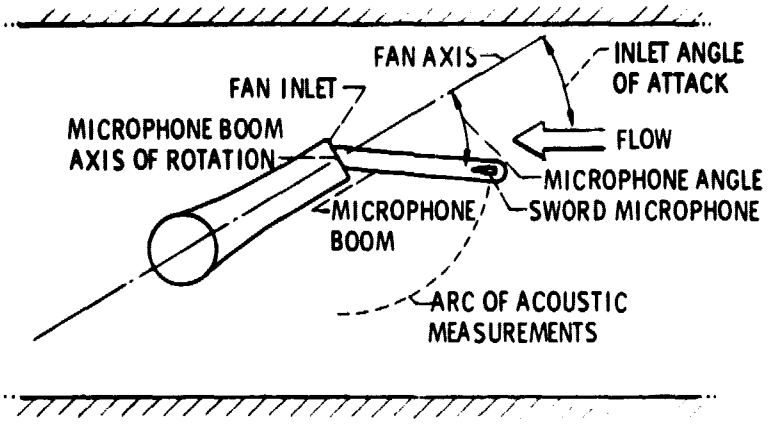

(b) SCHEMATIC PLAN VIEW.

Figure 2. - Concluded.

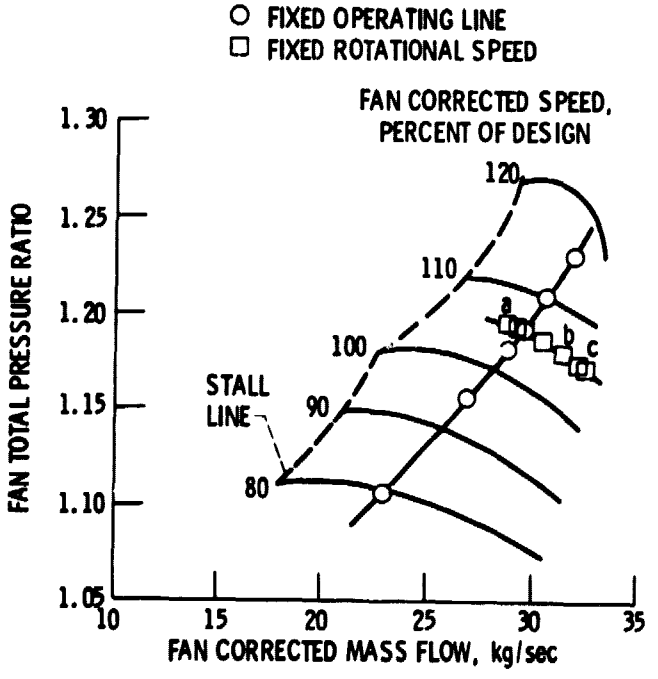

Figure 3. - Performance map for the model fan.

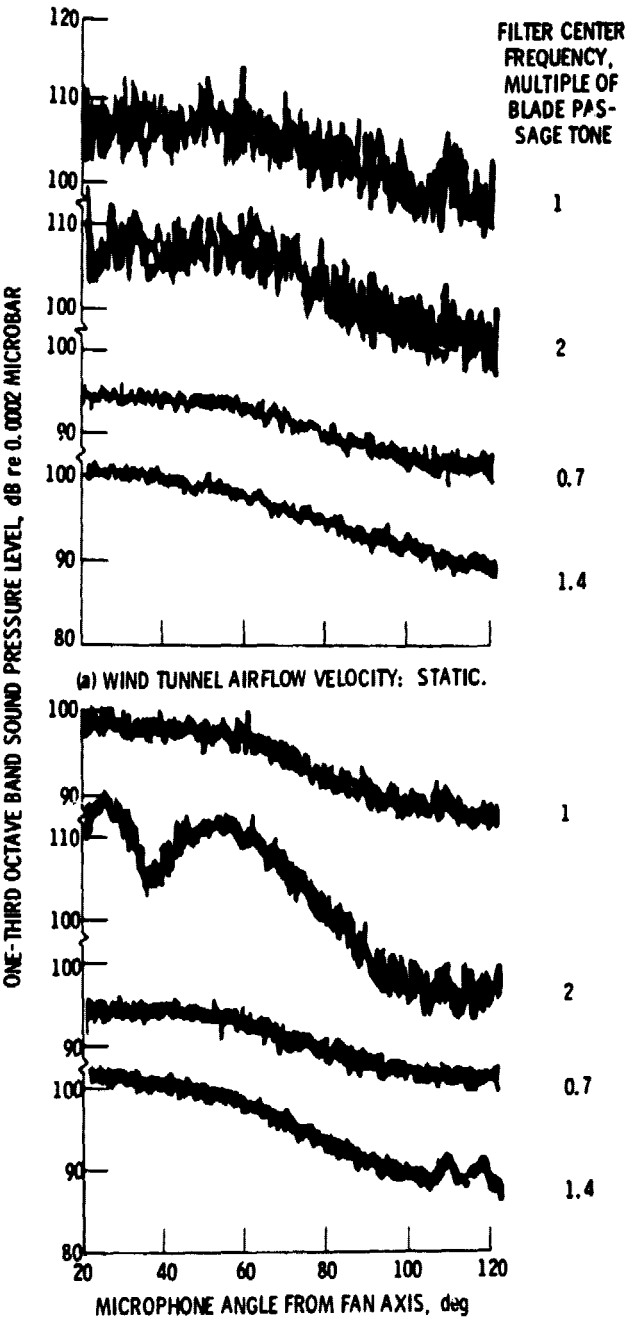

Figure 4. - Sound pressure level directivity of tone and broadband noise. Fan rotational speed: 95% of design. Inlet angle of attack; 0^{o}.

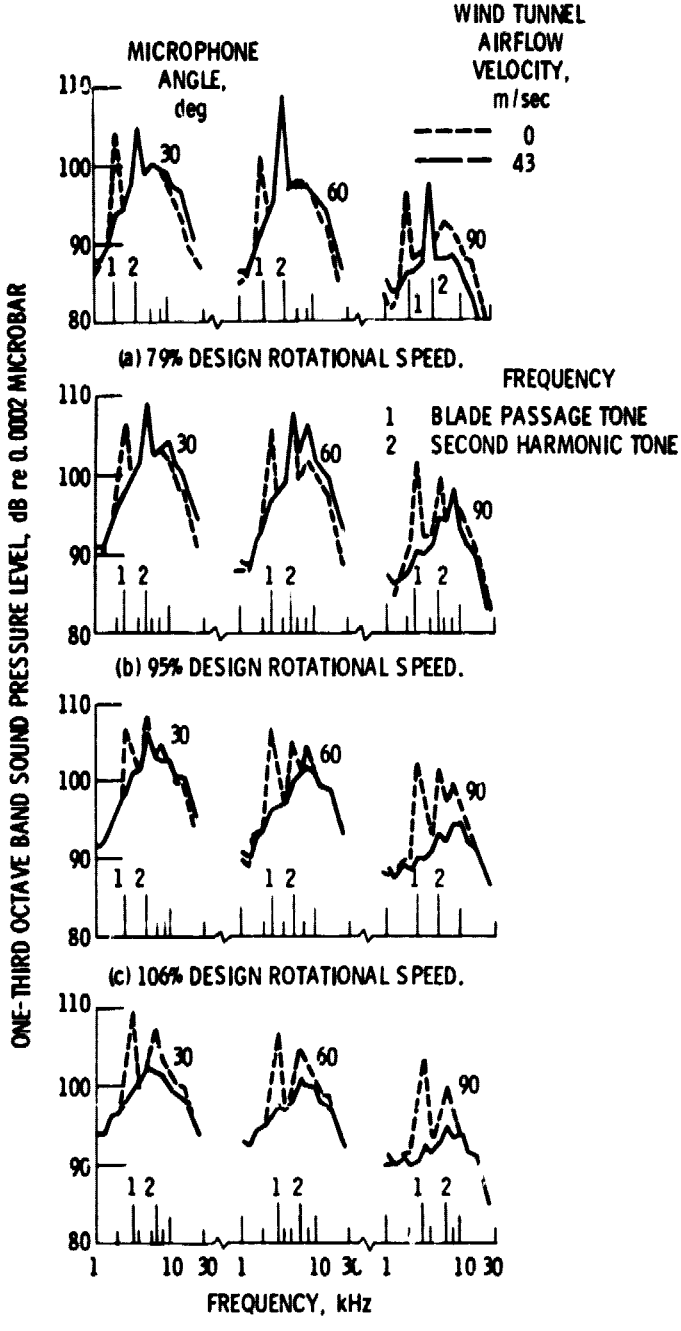

Figure 5. - One-third octave band sound pressure level spectra. Inlet angle of attack; 0^{0}.

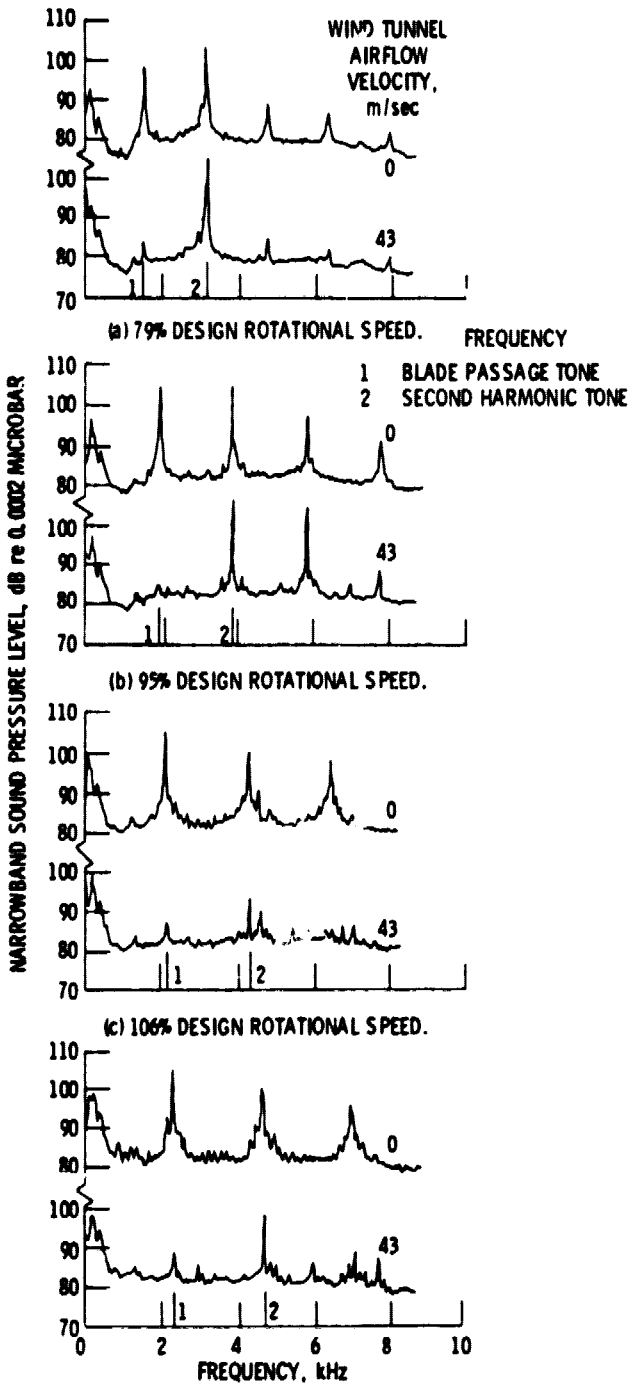

Figure 6. - Narrowband sound pressure level spectra. Inlet angle of attack; 0^{0}, microphone angle; 60^{0}.

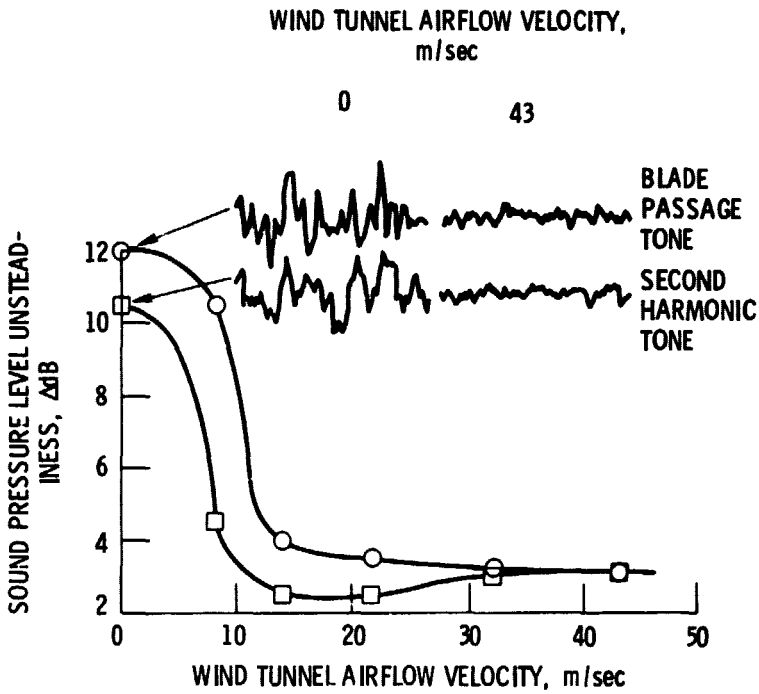

Figure 7. - Effect of forward velocity on tone unsteadiness at 95% design speed. Microphone angle; 60^{0}, Inlet angle of attack; 0^{0}.

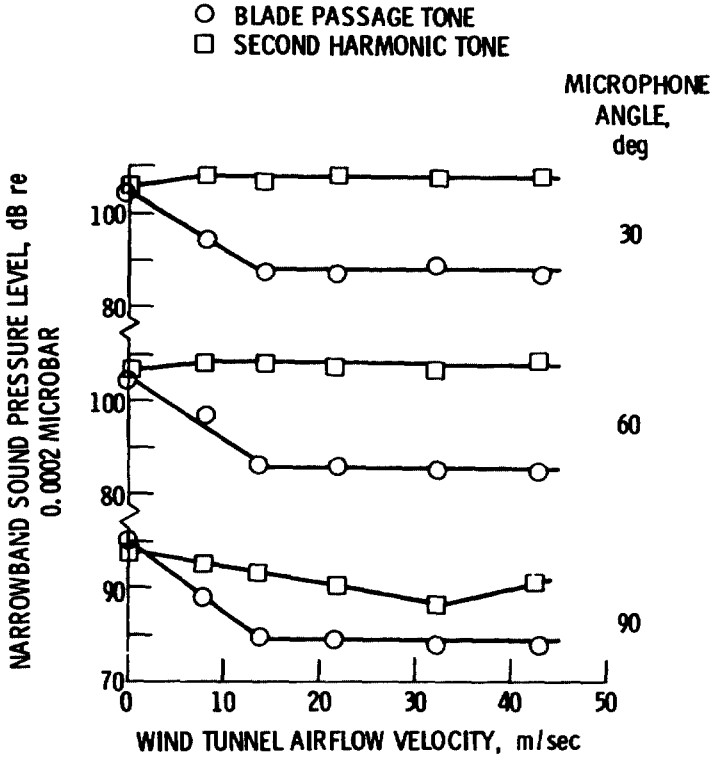

Figure 8. - Effect of forward velocity on sound pressure level at 95% design speed. Inlet angle of attack; 0^{0}.

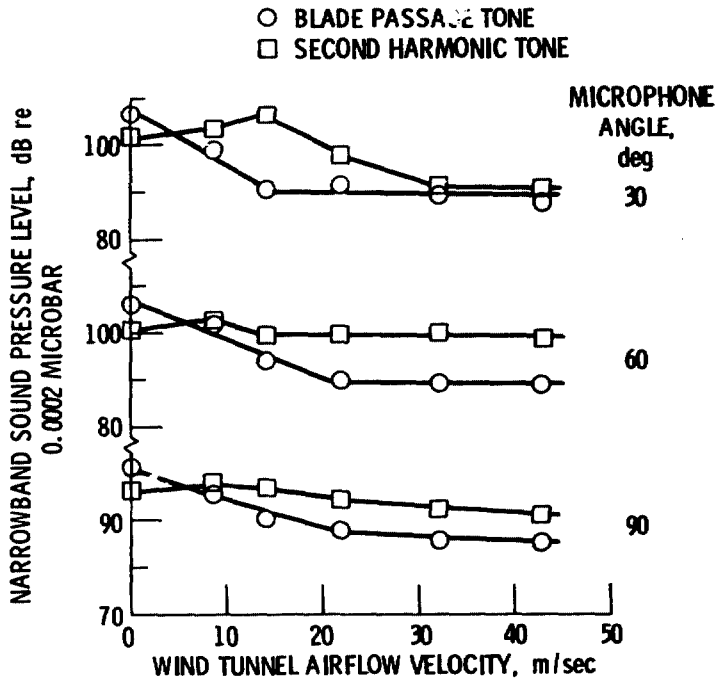

Figure 9. - Effect of forward velocity on sound pressure level at 116% design speed. Inlet angle of attack; 0^{0}.

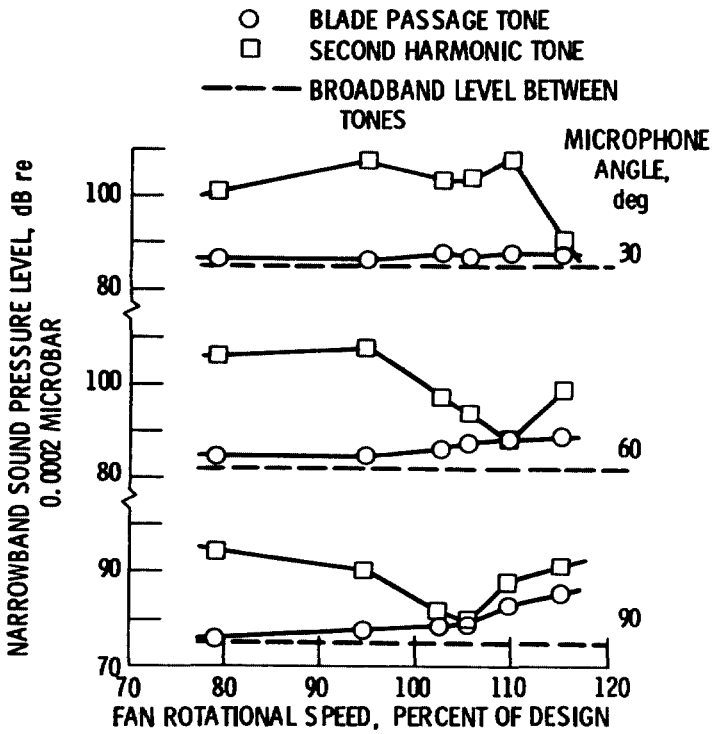

Figure 10. - Effect of fan rotational speed on sound pressure level at a tunnel velocity of 43 m/sec. Inlet angle of attack; 0^{o}.

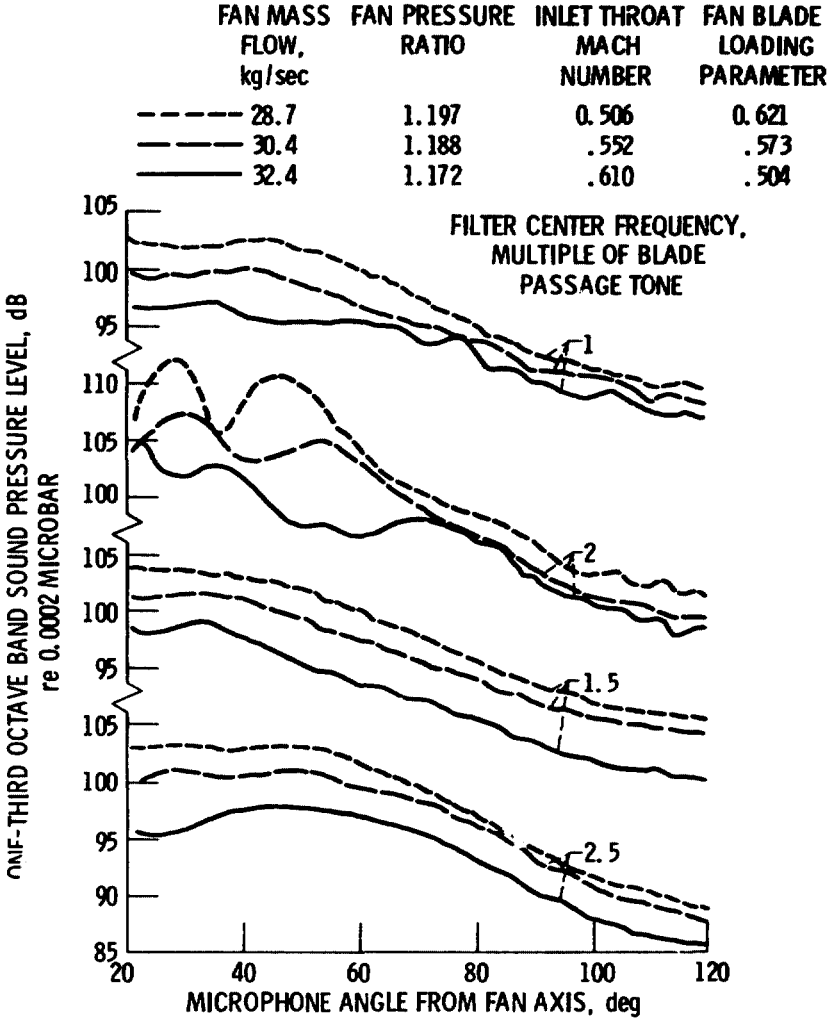

Figure 11. - Effect of fan blade loading on the sound pressure level directivity at a tunnel velocity of 43 m/sec and 106% design speed. Angle of attack; 0^{o}.

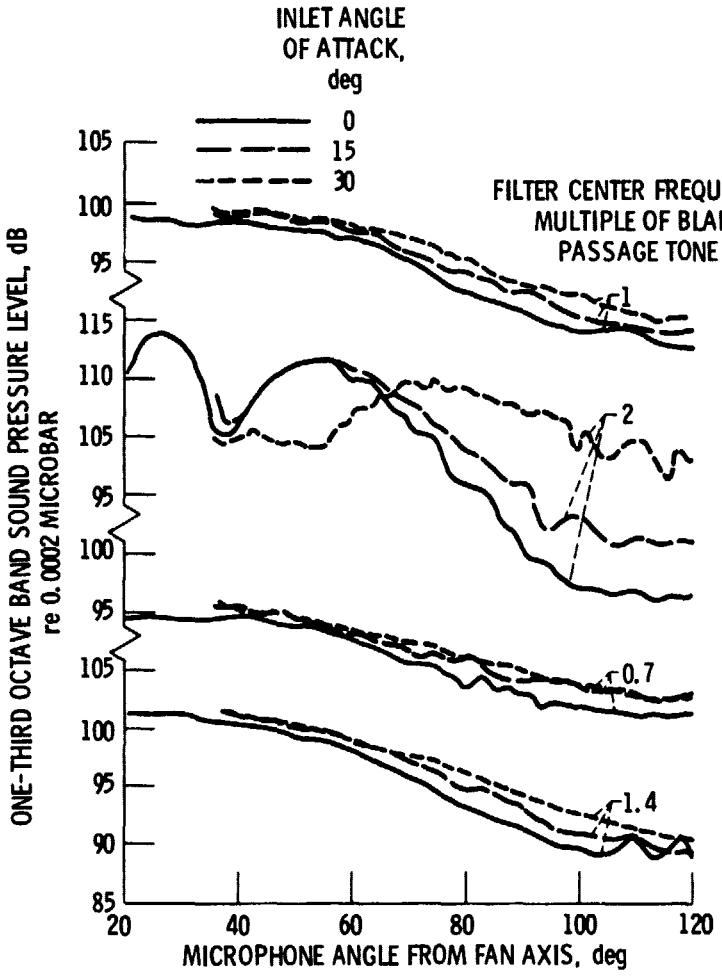

Figure 12. - Effect of angle of attack on the sound pressure level directivity at a tunnel velocity of 43 m/sec and 95% design speed.